

## ENTRAINMENT, MIXING, AND MICROPHYSICS IN TRADE-WIND CUMULUS

Hermann E. Gerber<sup>1</sup>, Glendon Frick<sup>1</sup>, Jorgen B. Jensen<sup>2</sup>, and James G. Hudson<sup>3</sup>

<sup>1</sup> Gerber Scientific Inc., Reston, VA, USA

<sup>2</sup> National Center for Atmospheric Research, Boulder, CO, USA

<sup>3</sup> Desert Research Institute, Reno, NV, USA

### 1. INTRODUCTION

A study of trade-wind cumulus clouds (Cu) observed during RICO from the NCAR C-130 research aircraft consists of analyzing the entrainment, mixing and microphysics of a conditionally-sampled set of 35 cumuli with active updraft cores penetrated during flight RF12. This study resembles the small-Cu study done by Raga et al (1990); however, the present study differs in that only those Cu are chosen for which the aircraft penetrated the core about 250-m below cloud top. The rationale for sampling in this updraft "bubble" near cloud-top of the Cu comes from the radar observations by Knight and Miller (1998) and Lasher-Trapp et al. (2003) which show that the first radar echo and subsequent precipitation are often observed in this region of actively growing small Cu. The aircraft flew predominately at 5 levels with 7 penetrations of individual clouds at each level chosen for the conditionally-sampled set. The sampling at 5 levels permit estimating the vertical evolution of this part of the Cu under the assumption that this sampling mimicked Lagrangian evolution.

The following summarizes the key findings for these Cu, and reports on the role of giant (GN) and ultra-giant (UGN) nuclei in causing the increasing amount of drizzle as a function of height in the Cu. A quasi-stochastic coalescence model is applied in a parcel model to predict the formation of the drizzle.

### 2. GENERAL DESCRIPTION OF THE Cu

The set of conditionally-sampled Cu range in height from ~400 m to ~1500 m, and their mean width at the 250-m level below cloud top is ~550 m as determined with the forward-looking digital video aboard the C-130. This relatively small width is similar to the width of the trade-wind Cu studied during BOMEX, but is significantly smaller than the "small" Cu in studies including such as CCOPE,

JHWRP, CaPE, and SCMS. The mean value of the vertical velocity in the RICO Cu is ~1.5 m/s, the bulk TKE dissipation rate is  $30 \text{ cm}^2/\text{s}^3$ , the fractional entrainment is  $1.3 \text{ km}^{-1}$ , with the latter value being identical to the value determined using a different sampling approach by Raga et al (1990) in the Hawaiian rain-band Cu (JHWRP).

The microphysical behavior of the 7 Cu at each of the 5 levels is shown in the following figures: Figure 1 shows the liquid water content (LWC; 1-hz data) measured with the PVM and 2D-C probes in all ~200 Cu penetrations on flight RF12. The preferred 5 levels flown by the aircraft are clearly shown. The data show that these Cu are strongly affected by entrainment, and that only a minimum amount of drizzle is observed by the 2D-C probe. The data also includes PVM LWC data (circles) collected at 1000 hz which show maximum LWC values about 25% larger than the 1-hz PVM data.

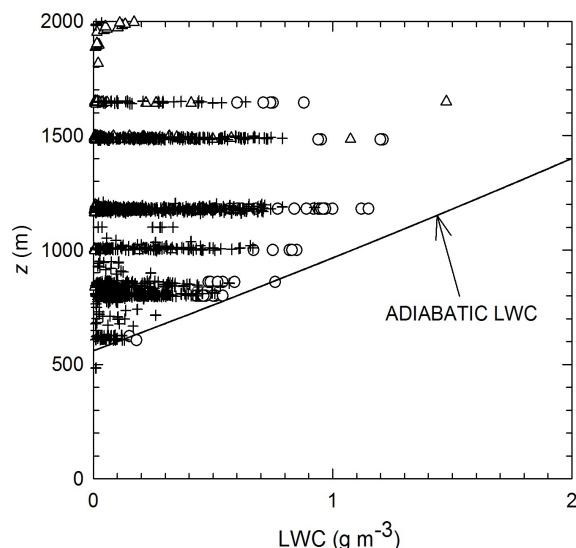


**Figure 1** - Liquid water content (LWC) measured at 1 hz for all ~200 Cu passes on RICO flight RF-12, PVM data (crosses), 2D-C data (triangles), 1000-hz PVM data (circles). Adiabatic LWC calculated from cloud base temperature, pressure.

Corresponding Author's Address: Dr. Hermann E. Gerber, GSI, 1643 Bentana Way, Reston, VA 20190, USA; Email: hgerber6@comcast.net

Figure 2 shows the average of the mean volume radius  $r_v$  for the 7 conditionally-sampled penetrations in individual Cu chosen at each of the 5 aircraft levels above cloud base and  $\sim 250$  m below cloud top. The calculated adiabatic  $r_v$  again illustrates the significant entrainment effect.

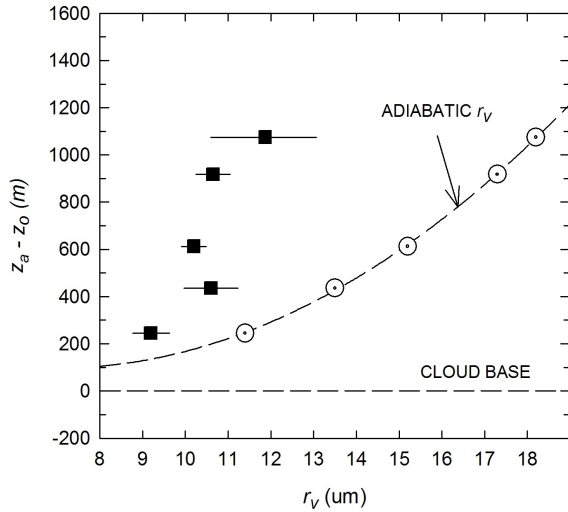


**Figure 2** - The average value of mean volume radius  $r_v$  (squares) for 7 conditionally-sampled Cu at each of 5 aircraft levels above cloud base ( $z_a - z_0$ ). Average adiabatic values of  $r_v$  calculated from mean measured droplet spectra in the Cu.

Figure 3 shows the mean droplet  $N$  and the cloud condensation nuclei  $CCN$  ( $S=1.5\%$ ) concentrations for the 7 Cu at the 5 levels above cloud base. Both parameters are approximately constant in the layer containing Cu, and the  $CCN$  constancy extends below and above this layer suggesting well-mixed conditions for the aerosol.

### 3. ENTRAINMENT AND MIXING

The  $\sim 10$ -cm incloud resolution 1000-hz PVM LWC and effective radius ( $R_e$ ) data are used to draw new inferences on the entrainment and mixing processes: The entrainment process involves smaller scales than previously thought; an example of depleted LWC parcels caused by entrained and observed during the aircraft pass into the edge of a Cu is shown in Fig.4. The length of the depleted parcels is lognormally distributed with a geometric mean length of 2.6 m.

The penetration depth of the depleted parcels is only several tens of m into the Cu which is consistent with the “mantle echoes” often observed

with radar by Knight and Miller (1998) in small Cu and attributed to sharp gradients in LWC and water vapor. The depleted parcels mix rapidly with the rest of the cloud given the measured TKE dissipation rate. This limits the appearance of “super-adiabatic” drops.

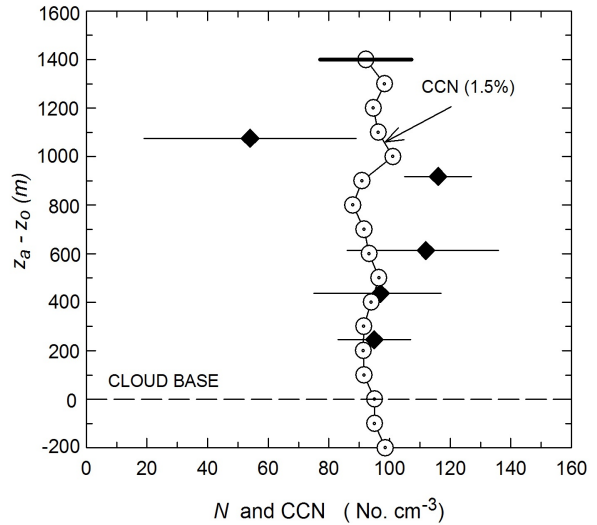


**Figure 3** - The average value of mean droplet concentration  $N$  for 7 Cu at each of 5 aircraft levels above cloud base ( $z_a - z_0$ ), and the average condensation nuclei concentration  $CCN$  at 1.5% supersaturation from aircraft profiles outside of cloud.

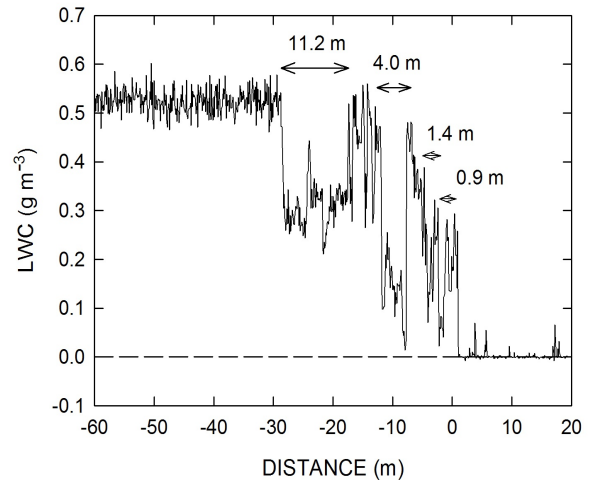


**Figure 4** - 10-cm resolution PVM LWC for a horizontal aircraft pass into the edge of a Cu. The location of arrows, defined as entrained parcels, represent the length of depleted LWC parcels with sharp gradients along both edges.

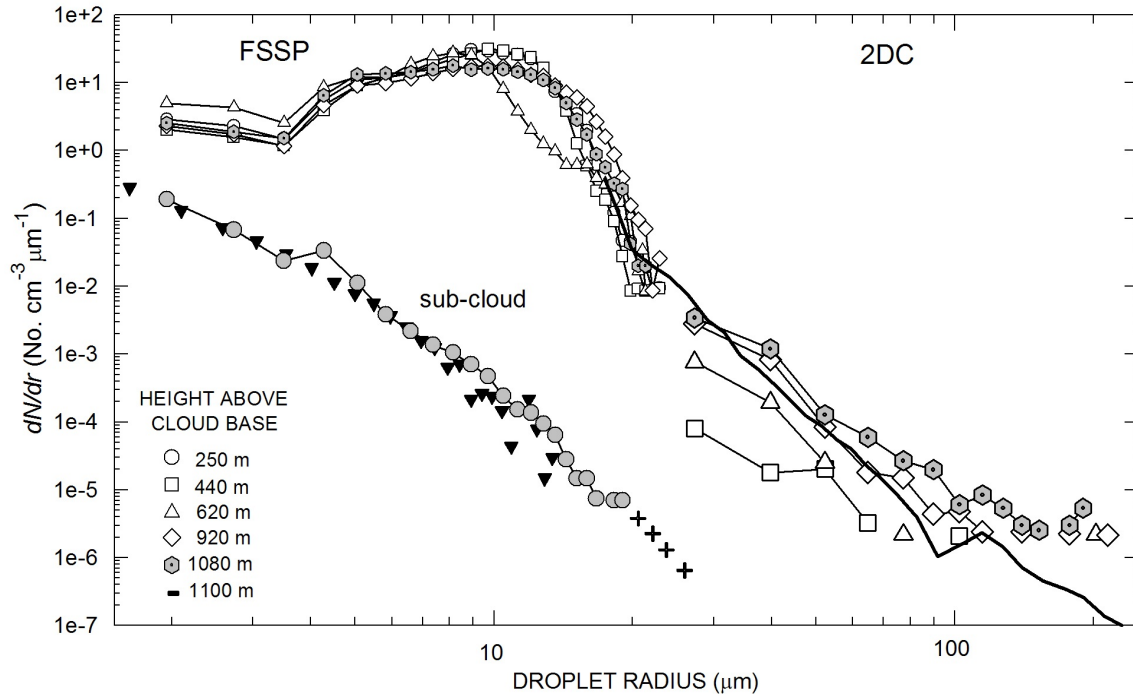


**Figure 5** - The average size distribution from 7 conditionally-sampled Cu of incloud droplets measured with the FSSP (small symbols), and incloud drizzle drops measured with the 2D-C probe (large symbols) at each of 5 levels above cloud base. The average subcloud FSSP spectrum (circles) is from the horizontal aircraft leg just below cloud base; and the NCAR GNI (Giant Nuclei Impactor; triangles, unpublished data) spectrum from the GNI dry sea-salt radii adjusted to the ambient RH = 86% in the leg. The solid curve is the parcel-model drizzle prediction for the top level (see text).

The incloud mixing following entrainment can be of three types, inhomogeneous extreme, inhomogeneous, and homogeneous (Jensen et al 1985). The evolution of the droplet spectra with height in the Cu is strongly dependent on which mechanism dominates as illustrated by Lasher-Trapp et al (2003). The 10-cm resolution LWC and Re PVM data show that the dominant mixing mechanism in these trade-wind Cu is either inhomogeneous extreme mixing or homogeneous mixing with entrained air that is near saturation. Both mechanisms cause primarily the dilution of the droplet concentrations without affecting the relative shape of the droplet size spectra, as also noted earlier, e.g., by Blyth and Latham (1990). Deviations from this behavior occur when the LWC in the cloud has been reduced by entrainment/mixing to small values and when new droplets are activated on CCN contained in the entrained air. The latter effect has a high correlation with the fractional entrainment that changes with height above cloud base.

#### 4. EVOLUTION OF DRIZZLE SPECTRA

A principal issue of RICO was to better understand the formation of precipitation in the trade-wind Cu, an issue that has a long unresolved history for warm clouds in general. The conditionally-sampled set of Cu for RF12 are used to address this issue. Figure 5 shows droplet size distributions measured in the Cu set using three probes, the 2D-C for drizzle-sized drops, the FSSP for incloud drops and subcloud particles smaller than ~45-μm diameter, and the GNI (Giant Nuclei Impactor; unpublished data provided by Jorgen Jensen) for collecting subcloud sea-salt particles on oil-coated slides exposed to the aircraft airstream. The GNI data is RH-adjusted to the ambient 86% RH of the subcloud aircraft leg to generate the GNI spectrum of salt-solution drops in Fig. 5 which shows reasonable agreement with the FSSP spectrum measured on the same pass. The dry size of the salt-solution drops is calculated using the droplet growth equation and results in spectra that follow Woodcock's (1953) dry sea-salt particle dependence on the Beaufort wind force. The FSSP droplet

spectra incloud are averages of the 7 Cu at each level (measured over ~100 m in the center of each Cu) and show a lack of variability with height above cloud base. The 2D-C spectra, on the other hand show a steady increase in drizzle-size drops with height.

The solid curve in Fig.5 is the predicted drizzle spectrum at cloud top resulting from a coalescence parcel model applied to the conditionally sampled set of Cu, using as initial conditions the quasi-steady incloud FSSP spectra as well as the subcloud FSSP sea-salt solution spectrum (for model details see Gerber et al, 2008). The calculations use a bin-less technique to avoid spectral broadening, and the collection efficiency used in the coalescence formulation (no inertial effects) follows the approach used by Cooper et al (1997). Reasonable agreement is found between the model prediction and the measured 2D-C spectrum at cloudtop. We find from the model results that the GN and UGN associated with the subcloud sea-salt solution drops play an essential role in generating the drizzle spectra for these Cu. The exposure of these sea-salt solution drops to saturated conditions in the cloud causes their relatively rapid growth to larger drops that then collect by accretion the smaller drops as measured with the FSSP; see Fig. 6. This behavior is similar to classical coalescence calculations (e.g., Berry and Reinhardt, 1974; Ochs, 1978).

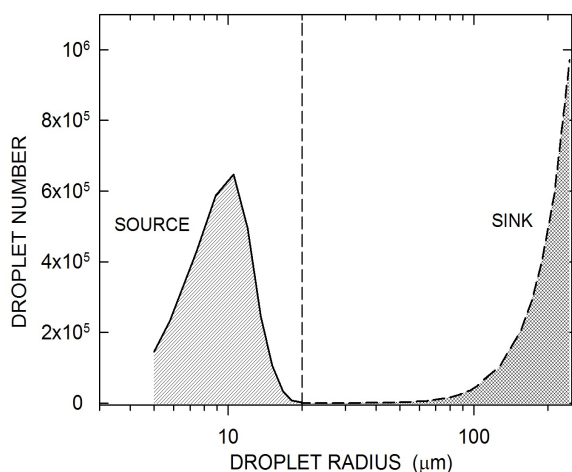


**Figure 6** - Predicted number of small drops lost by coalescence (source) to larger drops (sink) as a function of drop size for the 1100-m level above cloud base (see Fig. 5). The vertical dashed line indicates the radius 20 (um) that separates auto-conversion (smaller drops) from the accretion process.

## 5. FINDINGS

This quasi-Lagrangian study of the RICO trade-wind Cu from flight RF12 finds the entrainment, mixing, and microphysics behavior in the rising bubble of active turrets to be surprisingly uncomplicated. The entrained parcels are quite small, are likely related to the radar “mantle echoes” observed by Knight and Miller (1998), and are quickly mixed with the unaffected cloud preventing the presence of super-adiabatic drops. The mixing mechanism causes essentially only dilution of the droplets, the small droplet spectra remain approximately constant with height above cloud base, and the appearance of drizzle appears to follow the classical coalescence process. The wind generated sea-salt particles follow Woodcock’s (1953) wind speed dependence, and their presence is essential in collecting by accretion the small cloud drops to form the observed drizzle.

A surprising result is the approximate self-preserving nature of the small-droplet spectra as a function of height above cloud base. This behavior must represent an approximate balance between the gain of new droplets activating on CCN in entrained air, and losses of droplets by entrainment-dilution and by detrainment and coalescence. It is unknown if this simple behavior can be applied to other small Cu.

## ACKNOWLEDGMENTS

Thanks are due Bjorn Stevens, Robert Rauber, Harry Ochs, and Charlie Knight for organizing RICO. Appreciation is expressed to the Research Aviation Facility (RAF) of NCAR for their excellent running of RICO. This work was supported by NSF Grants ATM-0335695 and ATM-0342618.

## REFERENCES

- Berry, E.X., and R.L. Reinhardt, 1974: An analysis of cloud drop growth by collection. Parts I-IV. *J. Atmos. Sci.*, **31**, 1814-1831.
- Blyth, A.M., and J. Latham, 1990: Aircraft studies of altitudinal variability in the microphysical structure of non-precipitating, ice-free, Montana cumuli. *Quart.J. Roy. Meteor. Soc.*, **116**, 1405-1423.
- Cooper, W.A., R.T. Bruintjes, and G.K. Mather, 1997: Calculations pertaining to hygroscopic seeding with flares. *J. Appl. Meteor.*, **36**, 1449-1469.

Gerber, H., G. Frick, J.B. Jensen, and J.G. Hudson, 2008: Entrainment, mixing, and microphysics in trade-wind cumuli. *J. Meteor. Soc. Japan*, submitted.

Jensen, J.B., P.H. Austin, M.B. Baker, and A.M. Blyth, 1985: Turbulent mixing, spectral evolution and dynamics in a warm cumulus cloud. *J. Atmos. Sci.*, **42**, 173-192.

Knight, C.A., and R.A. Miller, 2007: Early radar echoes from small, warm cumulus: Bragg and hydrometeor scattering. *J. Atmos. Sci.*, **55**, 2974-2992.

Lasher-Trapp, S.G., W.A. Cooper, and A.M. Blyth, 2005: Broadening of droplet size distributions from entrainment and mixing in a cumulus cloud. *Quart. J. Roy. Meteor. Soc.*, **131**, 195-220.

Ochs, H.T., 1978: Moment-conserving techniques for warm cloud microphysical computations. Part II: Model testing and results. *J. Atmos. Sci.*, **35**, 1959-1973.

Raga, G.B., J.B. Jensen, and M.B. Baker, 1990: Characteristics of cumulus band clouds off the coast of Hawaii. *J. Atmos. Sci.*, **47**, 338-355.

Woodcock, A.H., 1953: Salt nuclei in marine air as a function of altitude and wind force. *J. Meteor.*, **10**, 362-371.